

REVISION 2

Mineral evolution and mineral niches of ammonium sulphates: the case of Pastora mine (Aliseda, Spain)

Ángel Crespo López¹, Carlos Pimentel^{2‡} and Carlos M. Pina^{1,3*}

¹*Departamento de Mineralogía y Petrología, Facultad de Ciencias Geológicas, Universidad Complutense de Madrid c/ José Antonio Novais, 2. E-28040 Madrid, Spain.*

²*Instituto Andaluz de Ciencias de la Tierra, Consejo Superior de Investigaciones Científicas, CSIC–Universidad de Granada, 18100 Armilla, Granada, Spain.*

³*Instituto de Geociencias IGEO (UCM – CSIC), E-28040 Madrid, Spain.*

[‡]*Present address: Univ. Grenoble Alpes, Univ. Savoie Mont Blanc, CNRS, IRD, Univ. Gustave Eiffel, ISTerre, 38000 Grenoble, France*

e-mail addresses: angelcre@ucm.es (A.C.), cpimentelguerra@geo.ucm.es (C.P.), cmpina@geo.ucm.es (C.M.P.),

**Corresponding author)*

Abstract

The uncommon association of ammonium sulphates identified in the Pastora abandoned mine is the result of a complex mineral evolution. By means of dissolution-(re)crystallisation reactions operating during large periods of time, ammonium minerals “adapt” to local spatio-temporal changes in physicochemical conditions. We found that during such an evolution, seasonal variations in temperature

and humidity, the relative solubility of mineral species, and the presence of organic matter play a fundamental role. In addition, our work shows the existence of “mineral niches” and “mineral seasonality”, which can be explained on the basis of the “mineral ecology” concept introduced by Hazen et al. (2015). Our investigation of the formation of hydrated sulphates, and particularly of ammonium sulphates, might be relevant to identify the existence of life in mineral formation environments.

KEYWORDS

Ammoniojarosite, tschermigite, acid mine drainage, dissolution-precipitation, mineral evolution.

Introduction

Even though hydrated and hydroxy sulphates are relatively frequent on Earth (sub)surface, the formation of sulphate minerals bearing ammonium is rare because concentrated ammonium-solutions are quite scarce in natural environments (Dutrizac and Jambor, 2000; Frost et al., 2006; Basciano, 2008). Bituminous slates, hot springs, solfataras, oil-bearing shales (Kampf et al., 2016), and sites related to coal deposits, as well as their remains after mining (e.g. coal-fire gas vents (Shimobayashi et al., 2011), and burning coal dumps (BCD) (Parafiniuk and Kruszewsk, 2009; Masalehdani et al., 2009)), are some of the few geological settings where ammonium sulphates are formed.

The occurrence of most ammonium sulphates seems to be mainly related to the weathering of sulfide minerals in a context of acid mine drainage (AMD) (e.g. Hammarstrom et al., 2005). However, the controlling factors of the precipitation and dissolution of these minerals under ambient conditions remain little known (Přikryl et al., 2007).

But the interest of ammonium sulphate minerals is not limited to their environmental implications. Since the identification on Mars of hydrated magnesium and iron sulphates, i.e. jarosite (Elwood Madden et al., 2004; Klingelhöfer et al., 2004), it becomes apparent that investigations on the formation of these minerals might be useful to detect possible aqueous environments on its surface (Spratt, 2015). In general terms, the occurrence of ammonium-bearing sulphates is relevant because the presence of organic matter seems to be a pre-requisite for the formation of ammonium minerals. Consequently, the detection of ammonium minerals can be considered as a circumstantial evidence of both aquatic environments and the presence of living organisms. In this regard, the abandoned Pastora iron mine has been revealed to be an outstanding natural laboratory in which numerous processes leading to the formation of a large variety of sulphate minerals can be studied (Crespo, 2015; Crespo et al., 2017, Crespo et al., 2017b). Particularly, Pastora mine provides a unique opportunity to analyse the main factors which determine the occurrence and the spatio-temporal distribution of ammonium sulphates under changing environmental conditions.

In this paper, we present an investigation of the formation of ammoniojarosite, $(\text{NH}_4)\text{Fe}_3(\text{SO}_4)_2(\text{OH})_6$, and tschermigite, $(\text{NH}_4)\text{Al}(\text{SO}_4)_2 \cdot 12\text{H}_2\text{O}$, in Pastora mine (Aliseda, Spain) from pre-existent sulphide minerals (i.e. pyrites). We found that, in the limited and to some extent controlled mineralogical environment of Pastora mine, the concepts of mineral evolution and mineral niches proposed by Hazen et al. (2008) are adequate to explain the generation of such minerals, which result from an intricate interplay between external (i.e. pH, temperature, relative humidity, interaction with host rocks and the supply of ammonium from organic origin) and internal factors (i.e. differences in solubility and stability of the minerals formed).

Geological context of Pastora mine

In the Sierra del Aljibe, approximately one kilometer south from Aliseda (Cáceres, SW Spain), there are several goethite and hematite mineral deposits. Some of them, including the abandoned Pastora iron mine, fulfilled the characteristics of gossan type ore deposits, i.e. mineral deposits originated by the weathering and oxidation of massive sulphides (mainly pyrite and marcasite) during their uplifting and exposure to the surface. Pastora mine is located in the north-western area of the Badajoz-Córdoba fault zone, within the Iberian Massif (Julivert et al., 1972). The Variscan or Hercynian orogeny was mainly responsible for the local geological structure, which shows wide antiformal structures affecting neoproterozoic materials (the so-called Schist Greywacke Complex), and narrow synclines where an almost complete sequence of the Paleozoic age can be observed (Soldevila, 1991). Most abandoned mine-sites such as Pastora Mine can be found in the North flank of Sierra de San Pedro syncline structure. Outcropping rocks are formed by an Ordovician to Permian detrital sedimentary sequence of quartzites, sandstones and slates (Crespo, 2015; Soldevila, 1992). In particular, Pastora mine is situated in Devonian quartzites and slates (Fig. 1).

Description of Pastora Mine

Pastora mine was intermittently exploited for the extraction of iron since early history until the mid-20th century (Crespo, 2015). The present study is focused on the two lowest levels of the mine where ammonium sulphates were identified. The sites where these sulphates are more abundant have been indicated in figure 2 (L1.S1 in level 1 and L2.S1 in level 2).

Level one (L1) is the lowest level and the main access to the mine. In L1, there are two small open areas at the entrance, connected by a short gallery, and followed by long galleries partially flooded (L1.S1). Level two (L2) is accessible from level one by means of a metal staircase, but it also has direct access from outside. While the external area of L2 is hardly sheltered from meteorical events, an intermediate zone (L2.S1), located before the underground galleries, is quite protected from weathering.

Materials and methods

X-Ray powder diffraction (XRPD)

Over one hundred mineral samples were collected from selected sites in Pastora Mine (galleries, shafts and open pits). Sampling was conducted for 3 years under different climatic and environmental conditions. After collection, mineral samples were packed into sealed plastic bags and stored at room temperature for subsequent analysis. Small fragments of the samples were gently crushed in an agate mortar and sieved to a particle size $<53 \mu\text{m}$ to be studied with X-ray powder diffraction. Diffraction was performed with a Siemens D-500 and a PANalytical X'Pert MPD diffractometers, both equipped with $\text{CuK}\alpha$ sources ($\lambda = 1.5405 \text{ \AA}$). This radiation was generated at 40 kV, 30 mA. Diffractograms were obtained with an angular step of $2\theta = 0.04^\circ$ with a time per step of 1 s, and the scan ranged from 2° to $90^\circ 2\theta$. Mineral phases present in the samples were identified by comparing the collected diffractograms with the PDF2 database using the X Powder software (Martin, 2008).

Scanning electron microscopy (SEM)

Among the samples examined by X-ray powder diffraction, 24 contained ammonium sulphates. These samples were selected to observe the morphology and habit of the crystals. They were coated with

gold and then examined and chemically analysed with a scanning electron microscopy (SEM, JEOL JSM 6400-40 kV). The acceleration voltage of the electron beam used was 20 kV with a current of 10 microamps, and 15 mm of working distance (scan time 20 μ sec/pixel).

Optical microscope

A number of selected fragments of the samples containing tschermigite and ammoniojarosite were mounted on glass slides to be further investigated with an optical microscope (Nikon Eclipse Ci POL), equipped with a camera Nikon D5500. Microphotographs were taken at magnifications of 50X, 100X and 200X.

Water analysis

Water sampling was conducted in a pond located at the entrance of the underground mine gallery (L1). Volumes of 120 cm³ of acid mine drainage (AMD) water were collected and stored in a sealed plastic tubes at room temperature. Prior to perform the chemical analyses, water samples were filtered with 0.2 μ m filters and acidified with nitric acid to a pH below 2. Then, they were analyzed by inductively coupled plasma optical emission spectrometry (ICP-OES) with a Spectro Arcos ICP-OES axial mode instrument. Blank and standards calibration solutions were prepared from SCP science 1000 ppm standards solutions. To calibrate the ICP-OES measurements mono-elemental 1000 mg/l Certipur Merck solutions for As, S and Si, and multi-element 1000 mg/l Certipur Merck IV standard solution for the rest of elements were used. Matrix reference material EnviroMAT Waste Water High (EU-H) and EnviroMAT Ground Water High (ES-H) were used for checking.

The concentration of ammonia was semiquantitatively determined using a visual colorimetric indophenol-hypochlorite method, based on the Berthelot reaction (Solorzano, 1969). The total ammonium nitrogen (TAN) is estimated carrying out the water to be analyzed to extremely alkaline condition, that is, without the presence of protons (H^+). In this way, all the ammonium ion (NH_4^+) in the water becomes ammonia (NH_3). The indophenol reagent colors the water from yellow to an intense blue color depending on the ammonia content and the TAN is estimated by comparison with a colorimetric scale (Loan et al., 2013). The detection limit of this method is 0.5 mg/L.

***In situ* measurements**

Temperature and pH of the acid drainage water was periodically measured *in situ* about every two months with a portable pH-meter with an accuracy of 0.01 pH units (Eutech Instruments, Eoscan) for a period of four years. Temperature and relative humidity data were recorded with two Easy log thermohygrometers simultaneous in level one (site L1.S1) and level 2 (site L2.S1) at least every one hour for a period of one year. In addition, data from the State Meteorology Agency (AEMET) collected at the automatic meteorological station, (ID 3562X, Aliseda (Cáceres) at latitude of 39° 25' 39" N., longitude of 6° 44' 11" W. and altitude of 321 m) were also compiled.

Results and discussion

Climatic conditions

As expected, external temperatures recorded at the AEMET station in Aliseda and temperatures measured inside the mine correlate (fig. 3a). However, differences between maximum and minimum temperatures inside the mine (ranging from 8°C in January to 17.5°C in August in L1S1 and ranging

from 9°C in January to 25°C in August in L2S1) are lower than outside (ranging from -6.5°C in January to 44°C in August). In addition, deeper galleries (L1.S1) are less affected by external temperature changes than sheltered zones before the galleries (L2.S1).

Rainfalls and relative humidity within the mine also correlate (fig. 3b). Nevertheless, there are significant differences between deeper galleries of level 1, where the maximum relative humidity ranges from 71% to 100%, and sheltered zones of level 2, where humidity ranges from 35% to 94.5%. Furthermore, average relative humidity values (L1.S1) are higher in deeper galleries than in sheltered areas (L2.S1).

Chemistry of mine water.

Although sulphur and some metal concentrations of Pastora mine waters are above typical values of local drinking waters (see Pantones River in Table 1), they are much lower than those measured in two representative AMD waters from Iberian Pyrite Belt (see Tinto and Odiel rivers in Table 1).

The Indophenol method showed that the content of TAN in the water samples was at least 10 mg/L (figure S11 of SI).

The values of pH of the waters are rather constant with an average value of 3.20 for the last four years with a minimum of 2.97 in November 2018 and a maximum of 3.49 in July 2018.

Ocurrence of sulphates in Pastora mine.

A remarkable diversity of mineral species has been identified in Pastora mine (Crespo, 2015; Crespo et al., 2017). Twenty of them, listed in Table 2, are sulphate minerals found in L1 and L2. Ammonium sulphates, ammoniojarosite, $[(\text{NH}_4)\text{Fe}_3(\text{SO}_4)_2(\text{OH})_6]$, and tschermigite,

$[(\text{NH}_4)\text{Al}(\text{SO}_4)_2 \cdot 12\text{H}_2\text{O}]$, formed under ambient conditions in Pastora mine and both are reported for the first time in an iron mine context.

While some of these sulphates, such as hexahydrate, rozenite, wattervilleite, epsomite, and even gypsum, are scarce, others such as copiapite (and other members of the copiapite magnesiocopiapite series), pickeringite, alunogen, fibroferrite, halotrichite, slavíkite and the two rare ammonium sulphates, tschermigite and ammoniojarosite, are relatively abundant.

Ammonium sulphates in Pastora mine

L2 and mainly in L1 of Pastora mine, ammonium sulphates cover large areas of walls and ceiling. They occur (i) on a dump matrix of kaolinitized wall-rocks with minor anatase (L1), (ii) on pervasively altered sandstone (L1), and (iii) on a matrix of gossanized goethite and hematite with minor amounts of disseminated pyrite (L1 and L2).

In the most samples with ammonium sulphates, ammoniojarosite occurs in association with tschermigite.

Figure 4 shows a diffractogram of a typical aggregate (sample PA107) of ammoniojarosite, covered by predominant tschermigite, from deep galleries (L1.S1) of Pastora mine. The sample is formed by a ~70.2 weight % of tschermigite and a ~29.8 weight % of ammoniojarosite (calculated using the reference intensity ratio (RIR) tool of the X Powder software for X-Ray diffraction data analysis; Hubbard and Snyder, 1988; Martín, 2008).

Ammoniojarosite $(\text{NH}_4)\text{Fe}_3(\text{SO}_4)_2(\text{OH})_6$. Ammoniojarosite crystallizes in the trigonal system (Basciano et al., 2007). In Pastora mine, it occurs as aggregates of subeuhedral to euhedral crystals yellow to pale brown which form globular masses and crusts on mine walls and ceiling.

A typical diffractogram of a sample, PA42, collected at L1 is showed in Figure SI2 of SI. This sample is composed of almost pure ammoniojarosite, ~93.2 weight %, with small amounts of kaolinite (RIR method; Hubbard and Snyder, 1988; Martín, 2008).

Table 1 in SI shows XRD data, values of d-spacing and relative intensities of this sample main diffractograms peaks, data are in good agreement with synthetic compound PDF number 26-1014. SEM images of this sample (Figure 5) show aggregates of randomly oriented ammoniojarosite crystals.

Tschermigite $(\text{NH}_4)\text{Al}(\text{SO}_4)_2 \cdot 12\text{H}_2\text{O}$. Tschermigite crystallizes in the isometric system (Abdeen et al., 1981). In Pastora mine, it appears as colourless aggregates forming efflorescences that usually cover crystals of ammoniojarosite (Figure 6). The aggregates are composed by imperfect octahedral crystals, up to 0.5 millimetre-size, with a vitreous lustre.

Table 2 in SI shows XRD data for tschermigite correspond to those for the ICDD-PDF 71-2203 compound which shows a good agreement with sample PA107.

Tables 3 and 4 show the different associations of ammonium minerals identified at level one and two, respectively. In both levels, ammonium sulphates appear together and in association with other sulphates (and also with other non-sulphate minerals).

Mineralization processes

The origin of iron, aluminium, ammonium, and ammonium sulphates

The pH of Pastora mine AMD waters ranges from 2.97 to 3.49. Such acid waters promote an intense chemical weathering of primary minerals and host-rocks. The sulphates identified at the mine, and their association with pyrite and hematite, confirm that they were formed under very acidic

conditions. In the case of ammonium sulphates, the biological activity of bats in Pastora mine also plays an important role in their formation.

In this respect, while sulphate ions and iron mainly come from the oxidation of pyrite contained in the slates, aluminium is mostly released from clays minerals such as kaolinite, which is ubiquitous in the mine (Dutrizac and Jambor, 2000; Crespo, 2015). In addition, the high concentration of ammonium ion in mine waters seems to be the result of the decomposition of organic matter (Dutrizac and Jambor, 2000; Frost et al., 2006). For instance, in the case of tschermigite formation in Lone Creek Fall Cave, ammonia comes from bat guano (Audra and Hoble'a, 2007). As far as the Pastora mine concerns, the large colony of greater horseshoe bats (*Rhinolophus ferrumequinum*) that roosts there is surely responsible for the high total ammonium nitrogen concentration measured in the mine water (>10mg/L). Considering the low pH values of the mine water, NH_4^+ ion is the predominant ammonium chemical species.

Frequently, ammonium sulphates are found as replacement after other K-bearing sulphates (Godeas and Litvak, 2006; Basciano, 2008). Thus, ammoniojarosite $(\text{NH}_4)\text{Fe}^{3+}_3(\text{SO}_4)_2(\text{OH})_6$ could have been formed after jarosite $(\text{KFe}^{3+}_3(\text{SO}_4)_2(\text{OH})_6)$; and tschermigite $(\text{NH}_4\text{Al}(\text{SO}_4)_2 \cdot 12\text{H}_2\text{O})$ after kalinite $(\text{KAl}(\text{SO}_4)_2 \cdot 12\text{H}_2\text{O})$. Moreover, tschermigite can be also formed by the hydration of the mineral godovikovite $(\text{NH}_4)\text{Al}(\text{SO}_4)_2$, through the following hydration reaction: $(\text{NH}_4)\text{Al}(\text{SO}_4)_2 \cdot 12\text{H}_2\text{O} \rightarrow (\text{NH}_4)\text{Al}(\text{SO}_4)_2 \cdot 12\text{H}_2\text{O}$ (Shimobayashi et al., 2011; Parainiuk and Kruszewski, 2009).

Alternatively, some ammonium sulphates can precipitate from aqueous solutions formed by weathering of sulfide minerals, the dissolution of sulphates previously formed and the incorporation of cations from external sources, i.e. K^+ and Al^{3+} from host rocks and NH_4^+ from biological activity (e.g. Hammarstrom et al., 2005; Parafiniuk and Kruszewski, 2009).

In Pastora mine, the ammoniojarosite-jarosite association has not been found so far. According to Dutrizac and Jambor (2000), there are two factors that favour the formation of jarosite, $\text{KFe}_3(\text{SO}_4)_2(\text{OH})_6$, rather than ammoniojarosite, $(\text{NH}_4)\text{Fe}_3(\text{SO}_4)_2(\text{OH})_6$: (i) the scarcity of NH_4^+ -rich solutions and (ii) the high $\text{K}^+ : \text{NH}_4^+$ ratios in natural waters. In Pastora mine, ammoniojarosite is predominant compared to jarosite. This is consistent with both the relatively high concentrations of NH_4^+ and the low $\text{K}^+ : \text{NH}_4^+$ ratios in the Pastora mine waters ($[\text{K}^+] = 7.0 \text{ mg/L}$; $[\text{NH}_4^+] > 10 \text{ mg/L}$, and $[\text{K}^+] : [\text{NH}_4^+] < 0.7$). These observations strongly suggest that ammoniojarosite did not replace jarosite crystals but it is most likely formed directly from NH_4^+ rich aqueous solutions.

With respect to the occurrence of tschermigite, it seems that this mineral did not form by any replacement process either. Tschermigite also appears as subeuhedral or euhedral crystals, and godovikovite has not been found anywhere in Pastora mine yet. This excludes kalinite and godovikovite as direct precursors of tschermigite. Therefore, tschermigite might precipitate directly from aqueous solutions.

Spatial and seasonal distribution of ammonium sulphates in Pastora mine

Given an adequate composition of the host rock (i.e. sulphides-bearing slates and sandstones) and the availability of ammonium ion from biological activity (i.e. from the horseshoe bats colony), the occurrence and stability of different sulphates and ammonium sulphates in specific sites in Pastora mine are mainly controlled by the following factors: (i) the relative solubility of sulphate minerals (jarosite, halotrichite, pickeringite, tschermigite, etc.), and (ii) the local climate conditions (i.e. temperature and humidity).

While most of the sulphates identified in Pastora mine are highly soluble in water (e.g. halotrichite, tschermigite), other sulphates such as gypsum, and jarosites, are significantly less soluble.

Within the jarosite group, ammoniojarosite, $(\text{NH}_4)\text{Fe}_3(\text{SO}_4)_2(\text{OH})_6$, has a similar solubility to that of gypsum ($K_{\text{sp, gyps}} \sim 10^{-4.59}$), and lower than that of hydroniumjarosite, $\text{H}_3\text{OFe}_3(\text{SO}_4)_2(\text{OH})_6$ ($K_{\text{sp, hjar}} \sim 10^{-5.39}$; Gynn, 2000; Basciano and Peterson, 2007).

This large difference in solubility of the sulphates together with the variations in environmental conditions can be invoked to explain the spatial and seasonal distribution of minerals in Pastora mine. Figure 7 shows zone A and zone B, at level 1 (a similar mineral spatial distribution can also be observed at level 2).

Zone A is more exposed to climatic conditions and, consequently, the most soluble sulphates (e.g. halotrichite, pickeringite or epsomite) are partially or completely dissolved during wet and cold months, while they re-precipitate in summer. Ammonium sulphates have not been found in this area due to both the quartzitic composition of the host rock and the lack of bat activity.

Differently, zone B is more sheltered, and it is only weakly affected by variations in temperature and humidity. In this zone, ammonium sulphates have been found (L1.S1 and L2.S1), and even tschermigite, a more soluble sulphate mineral than ammoniojarosite, persists all through the year.

The stable occurrence of tschermigite, and other highly soluble sulphates, such as pickeringite or minerals of the copiapite group in some areas of the deep galleries of level one (e.g. site L1.S1), is a distinctive characteristic of Pastora mine. There, walls and ceiling are completely damp throughout the year. Water ascension by capillarity is favored by a continuous flow of ground water and by the high relative humidity up to 100% in some periods of time (Přikryl et al., 2007; Hammarstrom et al., 2005). Olyphant et al. (1991) or Dold (1999) pointed-out that upwards migration of water by capillary is the dominant process in crusts of salts formation by evaporative events. Thus, ammonium sulphates are more abundant at this place, and they form efflorescences and aggregates of well-formed crystals of tschermigite growing on botryoidal aggregates, subeuhedral or euhedral crystals of ammoniojarosite.

According to Grigor'ev (1965) and Parafiniuk and Kruszewski (2009), the shape of mineral aggregates and crystals habits provide key information about mineral genesis. Large and well-developed crystals usually reveal slow crystallisation and recrystallization processes. Ammonium sulphates aggregates occurred at site L1.S1 in Pastora mine. This indicates that their formation is the result of cyclical dissolution (partial or complete) and slow (re)precipitation (Masalehdani et al., 2009). These processes occur at this site in a range of high relative humidity (71% to 100%) and at temperatures ranging only from 8°C (January) to 17.5°C (August). Interestingly, these conditions of high relative humidity and narrow range of temperature significantly differ from those of other geological environments where ammonium sulphates are commonly formed.

Mineral evolution and mineral niches of ammonium sulphates in Pastora mine

The idea of mineral evolution was first introduced in 1979 by Zhabin. In 1982, Yushkin reported an increase over time in the mineralogical variety on the Earth's surface (Yushkin, 1982). The observation of the increasing complexity of the mineral world from the beginning of the solar system gave raises some scientists to formulate the hypotheses that the number of mineral species in the solar system increased since its origin due to the evolution of physicochemical conditions. In an article published in 2008, Hazen and his collaborators, extended the concept of mineral evolution, proposing that throughout the Earth's history not only an increase in the number of minerals occurred but also the appearance of new mineral groups (Hazen et al., 2008). In this evolution, the rise of oxygen in the atmosphere and the development of biological process resulted in the emergence of numerous oxides and hydroxides, sulfates, phosphates and carbonates on the Earth's surface. Accordingly, Hazen et al. (2015) proposed that Earth's mineral evolution can be divided into several stages, each of which increased the mineral diversity of the planet as a consequence of local, regional, and global selective

processes. In this context, concepts of “habitable zones”, “habitability”, and “mineralogical niches” are relevant to explain the diversity and distribution of minerals in Earth’s crust (Hazen et al., 2015). Here we show that these concepts can also be applied to geological microenvironments such as Pastora mine, where several stages of mineral evolution can be identified (see Figure 8).

In Pastora mine, the first mineralization stage consisted in the hypogenous formation of pyrite, (1) in figure 8. Sulphides are relatively stable while they are underground. However, an exposition to air and water results in their oxidation, hydration and weathering, (2) in figure 8. These processes provide a primary source of Fe and they lead to the acidification of the environment, (3) in figure 8. In this physicochemical scenario, a second stage of mineral evolution can be recognized by the precipitation of typical gossan secondary minerals. In Pastora mine, this group of minerals includes the iron-containing oxyhydroxides and oxides goethite and hematite, (4) in figure 8. Reaction between water and pyrites release SO_4 ion and, in a third stage, simple hydrated salts are directly formed from cations contained in pyrite, e.g. rozenite ($\text{FeSO}_4 \cdot 4\text{H}_2\text{O}$), (5) in figure 8. At a subsequent fourth stage, the acid mine drainage (average $\text{pH} = 3.20$) further promotes both the weathering of host rocks and the leaching of cations, (6) in figure 8. This results in the formation of a wide suite of complex secondary sulphates of divalent and divalent–trivalent cations. Among them, alunogen ($\text{MgSO}_4 \cdot 7\text{H}_2\text{O}$), copiapite ($\text{Fe}^{2+}\text{Fe}^{3+}_4(\text{SO}_4)_6(\text{OH})_2 \cdot 20\text{H}_2\text{O}$), halotrichite ($\text{FeAl}_2(\text{SO}_4)_4 \cdot 22\text{H}_2\text{O}$), jarosite ($\text{KFe}^{3+}_3(\text{SO}_4)_2(\text{OH})_6$), slavíkite ($\text{Mg}_4\text{Fe}_{10}(\text{SO}_4)_{15}(\text{OH})_8 \cdot 13(\text{H}_2\text{O})$) and kalinite ($\text{KAl}(\text{SO}_4)_2 \cdot 12\text{H}_2\text{O}$), (7) in figure 8.

In Pastora mine, a fifth stage of mineral evolution related to biological activity has also been identified, (8) in figure 8. As pointed out by Hazen (2010), development of life is directly or indirectly responsible for the existence of a number of mineral species on the Earth’s surface. In the case of Pastora mine, the activity of a large colony of horseshoe bats (*Rhinolophus ferrumequinum*) provides an important source of ammonia, which permits the formation of ammoniojarosite, $(\text{NH}_4)\text{Fe}^{3+}_3(\text{SO}_4)_2(\text{OH})_6$,

and tschermigite, $(\text{NH}_4)\text{Al}(\text{SO}_4)_2 \cdot 12\text{H}_2\text{O}$, (9) in figure 8. Table 5 shows possible mineral reactions for each stage of mineral evolution described above. Nevertheless, further field and experimental work would be required to precisely determine such reactions.

Furthermore, the concepts of "habitable zones", "habitability" and "mineralogical niches" can be applied to the Pastora mine. Tschermigite and ammoniojarosite are two rare ammonium minerals with a quite limited "habitability zone", given their crystal chemical characteristics, they only appear in certain mineralogical niches where their conditions of formation and preservation, such as mineral stability ranges of temperature and relative humidity, are adequate.

Implications

Ammoniojarosite, $(\text{NH}_4)\text{Fe}_3(\text{SO}_4)_2(\text{OH})_6$, and tschermigite, $(\text{NH}_4)\text{Al}(\text{SO}_4)_2 \cdot 12\text{H}_2\text{O}$, have been identified in the abandoned Pastora iron mine, Aliseda (Cáceres, Spain). These minerals appear in association with other sulphates, and they form as a result of the oxidation of pyrite contained in slates and sandstones host-rocks. Their formation in Pastora mine is the result of complex processes in which acid mine drainage plays an important role. In addition, the NH_4^+ ion required for the precipitation of ammonium sulphates seems to be supplied by a large colony of greater horseshoe bats (*Rhinolophus ferrumequinum*) which roosts in Pastora mine. This paper shows that the formation of ammoniojarosite, tschermigite and associated sulphate minerals in Pastora mine is controlled by a series of dissolution-precipitation reactions responding to seasonal variations in ambient temperature and relative humidity. Accordingly, the observed association of ammonium sulphates can be considered as a stage of a mineral evolution in which new minerals crystallize and "adapt" to spatio-temporal changes in physicochemical conditions. In this sense, the concept of "mineral ecology" introduced by Hazen et al. (2015) is adequate

to interpret the diversity and distribution of sulphate minerals in Pastora mine. Furthermore, Pastora mine provides a unique opportunity to further investigate the formation of ammonium sulphates, a group of minerals, which to the best of our knowledge, had not been found in an iron mine to date. Our investigation of the formation of hydrated sulphates, and particularly of ammonium sulphates, might be relevant to identify potential conditions for the existence of life.

Acknowledgement

C. Pimentel acknowledges a Juan de la Cierva-Formación postdoctoral contract (ref. FJC2018-035820-I) from the Spanish Ministry of Science.

References

- Abdeen, A. M., Will G., Schafer W., Kirfel A., Bargouth M. O., Recker K., and Weiss A. (1981): X-ray and neutron diffraction study of alums II. The crystal structure of methylammonium aluminium alum III. *Zeitschrift fur Kristallographie*, V. 157, pp.147-166.
- Audra, P., and Hoble'a, F. (2007): The first cave occurrence of jurbanite $[Al(OH SO_4) 5H_2O]$, associated with alunogen $[Al_2(SO_4)_3 17H_2O]$ and tschermigite $[NH_4Al(SO_4)_2 12H_2O]$: thermal-sulfidic Serpents Cave, France. *Journal of Cave and Karst Studies*, V. 69(2), pp. 243–249.
- Basciano, L. C., and Peterson, R. C. (2007): The crystal structure of ammoniojarosite, $(NH_4)Fe_3(SO_4)_2(OH)_6$ and the crystal chemistry of the ammoniojarosite_hydrionium jarosite solid-solution series. *Mineralogical Magazine*, V. 71(4), pp. 427–441.
- Basciano L.C. (2008): Crystal chemistry of the jarosite group of minerals. Solid-solution and atomic structures. PhD thesis. Queen's University, Kingston, ON, Canada.

- Crespo, Á. (2015): La mina Pastora, Aliseda (Cáceres) como exponente del patrimonio geológico-minero de Extremadura. Trabajo Fin de Máster, Facultad de Geología, Universidad Complutense de Madrid.
- Crespo, Á., Pimentel C., Pedraz, P., and Pina, C. (2017): Caracterización y origen del sulfato eslavikita de la Mina Pastora, Aliseda (Cáceres). *Macla*. V. 22, pp 31-32.
- Crespo, Á., Pimentel, C., Pedraz, P., and Pina, C. (2017b): First occurrence of the rare mineral slavíkite in Spain, Aliseda (Cáceres). *Journal of Iberian Geology*. V. 43, pp 487-495.
- Dold, B. (1999): Mineralogical and geochemical changes of copper flotation tailings in relation to their original composition and climatic setting—implications for acid mine drainage and element mobility. Thesis. Université de Genève.
- Dutrizac, J. E., and Jambor, J.L. (2000): Jarosites and Their application in Hydrometallurgy. *Sulfate Minerals: Crystallography, Geochemistry, and Environmental Significance*. Edit: C.N. Alpers, J.L. Jambor, D.K. Nordstrom, 40(1): 405-452
- Elwood Madden, M., Bodnar, R., and Rimstidt, J. (2004): Jarosite as an indicator of water-limited chemical weathering on Mars. *Nature* 431: 821–823.
- Frost, R.L., Wills, R.A., Klopogge, J. T., and Martens, W. (2006): Thermal decomposition of ammoniumjarosite $(\text{NH}_4)\text{Fe}_3(\text{SO}_4)_2(\text{OH})_6$. *Journal of Thermal Analysis and Calorimetry*, V. 84 (2): 489–496.
- Godeas, M., and Litvak, V. (2006): Identificación de anomalías de amonio por espectrometría de reflectancia: implicancias para la exploración minera. Asociación Geológica Argentina. Buenos Aires. pp. 438-443.
- Grigor'ev, D. P. (1965): *Crystal Formation: Ontogeny of Minerals*. Translated from the Russian edition, 1961, by Israel Program for Scientific Translation. Y. Brenner, Ed. Davey, New York, 256 pp.

- Hammarstrom, J.M., Seal II, R.R., Meier, A.L., and Kornfeld, J.M. (2005): Secondary sulphate minerals associated with acid drainage in the eastern US: Recycling of metals and acidity in surficial environments. *Chemical Geology*, 215, 407-431.
- Hazen, R.M., Papineau, D., Bleeker, W., Downs, R.T., Ferry, J.M., McCoy, T.J., Sverjensky, D.A., and Yang, H. (2008): Mineral evolution. *American Mineralogist* 93: 1693-1720
- Hazen, R.M., Grew, E.S., Downs, R.T., Golden, J., and Hystad, G. (2015): Mineral ecology: Chance and necessity in the mineral diversity of terrestrial planets. *The Canadian Mineralogist*, 53(2):295.
- Hubbard, C.R., and Snyder, R.L. (1988): RIR-measurement and use in quantitative XRD. *Powder Diffraction* 3 (2), 74–77.
- I.G.M.E. Instituto Geológico y Minero de España (2020): Geological map number 703 (Arroyo de la Luz) (MAGNA).
- Julivert, M., Fontboté, J.M., Ribeiro, A., and Nabais-Conde, L.E. (1972). Mapa Tectónico de la Península Ibérica y Baleares 1:1.000.000. IGME.
- Kampf, A. R., Richards, R. P., Nash, B. P., Murowchick, J. B., and Rakovan, J. F. (2016): Carlsonite, $(\text{NH}_4)_5\text{Fe}^{3+}_3\text{O}(\text{SO}_4)_6 \cdot 7\text{H}_2\text{O}$, and huizingite-(Al), $(\text{NH}_4)_9\text{Al}_3(\text{SO}_4)_8(\text{OH})_2 \cdot 4\text{H}_2\text{O}$, two new minerals from a natural fire in an oil-bearing shale near Milan, Ohio. *American Mineralogist*, 101(9), pp. 2095-2107
- Klingelhöfer, G., Morris, R.V., Bernhardt, B., Schröder, C., Rodionov, D.S., de Souza, P.A. Jr, Yen, A., Gellert, R., Evlanov, E.N., Zubkov, B., Foh, J., Bonnes, U., Kankeleit, E., Gütlich, P., Ming, D.W., Renz, F., Wdowiak, T., Squyres, S.W., and Arvidson, R.E. (2004) Jarosite and hematite at Meridiani Planum from Opportunity's Mossbauer Spectrometer. *Science* 306(5702):1740-5.

- Loan, D.K., Con, T.H., Hong, T.T., and Mai Ly, L.T. (2013): Quick Determination of Ammonia Ions in Water Environment Based on Thymol Color Creating Reaction. *Environmental Sciences*, Vol. 1 (2): 83 – 92.
- Martín, J. D. (2008): Programa para el análisis por difracción de rayos X. *Métodos de polvo* (in Spanish).
- Masalehdani, M.N.N., Mees, F., Dubois, M., Coquinot, Y., Potdevin, J.L., Fialin, M., and Blanc-Valleron, M.M. (2009): Condensate minerals from a burning coal-waste heap in Avion, Northern France. *The Canadian Mineralogist*, Vol. 47: 573-591.
- Mitchell, R. E. (2002). Mechanisms of pyrite oxidation to non-slugging species. Stanford University (US).
- Olías, M., Nieto, J. M., Sarmiento, A. M., and Cánovas, C. (2010): La contaminación minera de los ríos Tinto y Odiel. Universidad de Huelva, Huelva, 166 pp (in Spanish).
- Olyphant, G.A., Bayless, G.R., and Harper, D. (1991): Seasonal and weather-related controls on solute concentrations and acid drainage from a pyritic coal-refuse deposit in southwestern Indiana, USA. *Journal of Contaminant Hydrology* 7: 219–236.
- Parafiniuk, J., and Kruszewski, Ł. (2009): Ammonium minerals from burning coal-dumps of the Upper Silesian Coal Basin (Poland). *Geological Quarterly*, 53, 341-356.
- Přikryl, R., Melounová, L., and Vařilová, Z. (2007): Spatial relationships of salt distribution and related physical changes of underlying rocks on naturally weathered sandstone exposures (Bohemian Switzerland National Park, Czech Republic). *Environmental Geology* 52: 409–420.
- Shimobayashi, N., Ohnishi, M., and Miura, H. (2011): Ammonium sulphate minerals from Mikasa, Hokkaido, Japan: boussingaultite, godovikovite, efremovite and tschermigite. *Journal of Mineralogical and Petrological Sciences*. Volume 106: 158–163.

- Soldevila i Bartolí, J. (1991): “Estudio geológico-estructural de los materiales precámbricos y paleozoicos entre la Sierra de San Pedro y la Depresión del Guadiana (provincias de Cáceres y Badajoz). Sector límite entre las zonas Centroibérica y Ossa-Morena”. Tesis Doctoral, Universidad Autónoma de Barcelona, 262 pp.
- Soldevila i Bartolí, J. (1992): “La sucesión paleozoica en el Sinforme de la Sierra de San Pedro (provincias de Cáceres y Badajoz, SO de España)”. *Estudios geológicos*, 48: 363-379.
- Spratt, H.J., (2015): Structural effects of ammonium and hydronium in jarosite minerals. PhD School of Chemistry, Physics and Mechanical Engineering. Queensland University of Technology.
- Solorzano, L. (1969): Determination of ammonia in natural waters by the phenolhypochlorite method. *Limnology and Oceanography*, vol.14(5), pp.799–801.
- Warr, L.N. (2021). IMA–CNMNC approved mineral symbols. *Mineralogical Magazine*, 85(3), 291-320.

List of figure captions

Figure 1. Geological location of the mine sites in the Upper Devonian. Or: Ordovician. Quartzites, slates and sandstones. Si: Siluric. Grey quartzites, black slates and sandstones. DL: Lower Devonian. Quartzites, ferroginous sandstones and slates. DM-DU: Middle Devonian - Upper Devonian. Quartzites and slates. DU,Q: Upper Devonian. Quartzites (Aljibe). DU,S: Upper Devonian. Slates, sandstones and quartzites. Ho: Holocene. Debris flow. Angular pebbles. Main mining works have been marked with the symbol of abandoned mining site. Figure modified after geological map number 703 (Arroyo de la Luz) (MAGNA). Instituto Geológico y Minero de España (I.G.M.E), 2020.

Figure 2. Pastora mine plan and longitudinal section (levels one and two). (Not to scale).

Figure 3. Monthly evolution of (a) average temperature, and (b) relative humidity and rainfall. Data recorded in levels 1 and 2 compared with external data from the meteorological station ID 3562X, located in Aliseda.

Figure 4. Diffractogram of sample PA-107, collected at level 1. In this sample, tschermigite occurs in assemblage with ammoniojarosite. Vertical solid lines indicate the positions and relative intensities of tschermigite (Tmi) (PDF number 71-2203). Vertical dotted lines indicate the positions of the peaks of ammoniojarosite (Ajrs) (PDF number 26-1014).

Figure 5. SEM images of aggregates of ammoniojarosite euhedral crystals, sample PA42, from level 1.

Figure 6. Optical microscope image of sample PA107 showing imperfect transparent octahedral crystals of tschermigite (Tmi) growing on pale yellow ammoniojarosite (Ajrs). Magnification 50x.

Figure 7. Schematic cross-section of level 1. Zones with different chemical and environmental conditions.

Figure 8. Mineral evolution increases mineral species at Pastora mine (simplified schema). Grey boxes: different stages: (1) first stage, hypogenous mineralization; (4) second stage, minerals formation by weathering of pyrite; (5) third stage, simple divalent hydrated salts formation from pyrite; (7) fourth stage, minerals formation by leaching of host rocks cations; (9) fifth stage, new minerals formation due to biological activity. The process results in an increase in mineral species.

Deposited items

This work includes a supplementary material with 2 figures and 2 tables.

Tables

Table 1. Chemical analyses of AMD of Pastora mine compared with the results of previous analyses of other representative AMD waters (Tinto and Odiel) and drinking water from that area (Pantones river). Concentrations in mg/l.

	Pastora mine* (Aliseda)	Tinto River** (Niebla)	Odiel River** (Gibraleón)	Pantones River*** (Arroyo de la Luz)
Temperature (°C)	15	19	18	—
pH	3.5	2.8	3.6	8.9
Aluminum	4	77	37	< 0.2
Arsenic	0.007	0.202	0.013	< 0.02
Sulphur	66	224	712	< 10
Calcium	4.8	73	50	< 5.0
Cobalt	0.048	0.558	288	< 0.01
Copper	0.011	19	5.4	< 0.01
Iron	6	157	7.5	< 0.05
Lithium	0.032	0.137	79	—
Magnesium	9.6	76	72	< 5.0
Manganese	1.8	7.8	8.5	< 0.01
Nickel	0.039	0.175	152	< 2.0
Potassium	7.0	3.9	2.8	< 2.5
Sodium	12	38	21	8.5
Silicon	5.2	15	14	—
Zinc	0.063	24	13	< 0.02

* Crespo (2015) **Olías et al., (2010) ***Data (2014.05.28) from Tajo Hydrographic Confederation.

Table 2. Sulphates identified in Pastora mine. Ammonio sulphates, ammoniojarosite and tschermigite, are highlighted in this table. (*) (Formula proposed by Crespo et al. 2017).

Sulphate mineral	Chemical formulae	Description	Level
Aluminocopiapite	$\text{Al}_{2/3}\text{Fe}^{3+}_4(\text{SO}_4)_6(\text{OH})_2 \cdot 20\text{H}_2\text{O}$	Yellow masses usually on the floor	L2
Alunogen	$\text{Al}_2(\text{SO}_4)_3 \cdot 17\text{H}_2\text{O}$	White masses	L2
Ammoniojarosite	$(\text{NH}_4)\text{Fe}_3(\text{SO}_4)_2(\text{OH})_6$	Yellow masses and crust covering walls and ceiling	L1-L2
Apjohnite	$\text{Mn}^{2+}\text{Al}_2(\text{SO}_4)_4 \cdot 22\text{H}_2\text{O}$	Associated with halotrichite as white globular masses	L1
Copiapite	$\text{Fe}^{2+}\text{Fe}^{3+}_4(\text{SO}_4)_6(\text{OH})_2 \cdot 20\text{H}_2\text{O}$	Yellow masses	L2
Dorallcharite	$\text{TiFe}_3^{+3}(\text{SO}_4)_2(\text{OH})_6$	Associated with ammoniojarosite on goethite	L2
Epsomite	$\text{MgSO}_4 \cdot 7\text{H}_2\text{O}$	Colorless to white fibrous masses associated with wattevilleite	L1
Ferricopiapite	$\text{Fe}^{3+}_{0.67}\text{Fe}^{3+}_4(\text{SO}_4)_6(\text{OH})_2 \cdot 20\text{H}_2\text{O}$	Yellow masses usually on the floor	L2
Fibroferrite	$\text{Fe}^{3+}(\text{SO}_4)(\text{OH}) \cdot 5\text{H}_2\text{O}$	Pale brown crust on the walls	L2
Gypsum	$\text{CaSO}_4 \cdot 2\text{H}_2\text{O}$	Efflorescences on the walls	L1-L2
Halotrichite	$\text{FeAl}_2(\text{SO}_4)_4 \cdot 22\text{H}_2\text{O}$	Associated with pickeringite as white globular masses usually on the floor	L1-L2
Hexahydrate	$\text{MgSO}_4 \cdot 6\text{H}_2\text{O}$	White masses on quartzitic	L1

		walls	
Jarosite	$\text{KFe}^{3+}_3(\text{SO}_4)_2(\text{OH})_6$	Yellow crusts on goethite	L1-L2
Kalinite	$\text{KAl}(\text{SO}_4)_2 \cdot 12\text{H}_2\text{O}$	In assemblage with pickeringite and halotrichite	L1-L2
Magnesiocopiapite	$\text{MgFe}^{3+}_4(\text{SO}_4)_6(\text{OH})_2 \cdot 20\text{H}_2\text{O}$	Yellow masses usually on the floor	L2
Pickeringite	$\text{MgAl}_2(\text{SO}_4)_4 \cdot 22\text{H}_2\text{O}$	Associated with halotrichite as white globular masses	L1-L2
Rozenite	$\text{FeSO}_4 \cdot 4\text{H}_2\text{O}$	Associated with copiapite and ammonio sulphates	L2
Slavíkite	$\text{Mg}_4\text{Fe}_{10}(\text{SO}_4)_{15}(\text{OH})_8 \cdot 13(\text{H}_2\text{O})^*$	Yellow powder crust on the walls	L2
Tschermigite	$(\text{NH}_4)\text{Al}(\text{SO}_4)_2 \cdot 12\text{H}_2\text{O}$	Colorless efflorescences with vitreous luster usually covering ammoniojarosite	L1-L2
Wattevilleite	$\text{Na}_2\text{Ca}(\text{SO}_4)_2 \cdot 4\text{H}_2\text{O}(?)$	Colorless to white fibrous masses associated with epsomite	L1

Table 3. Association of ammonium minerals identified at level one. Tschermigite (Tmi), ammoniojarosite (Ajrs), kalinite (Kli), slavikite (Svi), jarosita (Jrs), gypsum (Gp), copiapite group (Cpi), fibroferrite (Ffr), rozenite (Rzn), alunogen (Alg), dorallcharite (Dcr), Other (Oth). Zone: Sheltered zone (SZ), Deep gallery (DG). Numbers are weight percentages of the identified phases calculated from the diffractograms using the RIR method (Hubbard and Snyder, 1988; Martín, 2008). All abbreviations are accordingly to IMA-CNMNC approved mineral symbols (Warr, 2021).

Sample	Form of occurrence	Date of collect	Zone	Tmi	Ajrs	Kli	Svi	Jrs	Gp	Cpi	Ffr	Rzn	Alg	Drc	Oth
PA42	Crusts	2015-04-12	SZ		93.2										6.8
PA133	Crusts	2018-05-02	SZ	76.0	24.0										
PA109	Efflorescences	2017-08-09	DG	85.1	14.9										
PA107	Efflorescences	2017-08-09	DG	70.2	29.8										
PA100	Efflorescences	2016-12-17	DG	33.3	66.7										
PA132	Powder crust	2018-05-02	SZ	76.3				23.7							
PA119	Efflorescences	2017-11-11	DG	32.3						16.2	51.5				
PA108	Efflorescences	2017-08-09	DG	40.8	50.2							8.9			
PA121	Efflorescences	2017-11-11	DG	64.7	14.5				14.5						
PA143	Crust	2020-07-26	SZ	30.9	69.1										
PA144	Efflorescences	2020-07-26	DG	65.0				12.9	22.1						
PA145	Efflorescences	2020-08-01	DG	75.6				24.4							
PA151	Globular masses	2020-10-11	DG	69.2	30.8										
PA152	Globular masses	2020-10-11	DG	47.2				3.5			30.9				18.4

Table 4. Association of ammonium minerals identified at level two. Tschermigite (Tmi), ammoniojarosite (Ajs), kalinite (Kli), slavíkite (Svi), jarosita (Jrs), gypsum (Gp), copiapite group (Cpi), fibroferrite (Ffr), rozenite (Rzn), alunogen (Alg), dorallcharite (Drc), Other (Oth). Zone: Sheltered zone (SZ), Deep gallery (DG). Numbers are weight percentages of the identified phases calculated from the diffractograms using the RIR method (Hubbard and Snyder, 1988; Martín, 2008). All abbreviations are accordingly to IMA-CNMNC approved mineral symbols (Warr, 2021).

Sample	Form of occurrence	Date of collect	Zone	Tmi	Ajs	Kli	Svi	Jrs	Gp	Cpi	Ffr	Rzn	Alg	Drc	Oth
PA13	Powder crust	2015-09-03	SZ	10.1			89.9								
PA13A	Powder crust	2016-03-21	SZ	10.6	36.4		53.0								
PA13B	Powder crust	2016-05-03	SZ	7.9	32.9		59.2								
PA13C	Powder crust	2017-03-14	SZ	13.8			86.2								
PA79	Crusts	2016-03-21	SZ		87.1									9.0	3.9
PA82	Powder crust	2016-08-25	SZ	50.8	49.2										
PA85	Crusts	2016-08-25	DG	33.3			31.2			35.5					
PA146	Powder crust	2020-09-05	SZ	32.5		34.3									33.2
PA147	Powder crust	2020-09-05	SZ	29.0			71.0								
PA150	Crust	2020-08-01	DG	12.3	8.2					3.9			18.1		57.5

Table 5. Possible mineral reactions for each stage of mineral evolution in Pastora mine (see explanation in the main text).

Stage	Mineral phases and chemical formulae	Possible mineral reaction*	Observations
First	Pyrite S ₂ Fe	$[S_2]^{2-} + Fe^{2+} \rightarrow FeS_2$	Pyrite oxidation produces Fe ²⁺ and SO ₄ ²⁻
Second	Goethite FeOOH	$Fe^{3+} + 2 H_2O \rightarrow FeOOH + 3H^+$	Fe ³⁺ from Fe ²⁺ oxidation
	Hematite Fe ₂ O ₃	$FeS_2 \rightarrow FeS \rightarrow FeO \rightarrow Fe_3O_4 \rightarrow Fe_2O_3$	Pyrite oxidizes according to this reaction sequence**
Third	Rozenite Fe ²⁺ SO ₄ ·4H ₂ O	$Fe^{2+} + SO_4^{2-} + 4H_2O \rightarrow Fe^{2+}SO_4 \cdot 4H_2O$	Fe ²⁺ and SO ₄ ²⁻ ions released from pyrite
Fourth	Jarosite KFe ³⁺ ₃ (SO ₄) ₂ (OH) ₆	$3Fe^{3+} + 2SO_4^{2-} + K^+ + 6H_2O \rightarrow KFe^{3+}_3(SO_4)_2(OH)_6 + 6H^+$	SO ₄ ²⁻ and Fe released from pyrite, and K ⁺ from host rock
	Kalinite KAl(SO ₄) ₂ ·12H ₂ O	$Al^{3+} + K^+ + 2SO_4^{2-} + 12H_2O \rightarrow KAl(SO_4)_2 \cdot 12H_2O$	SO ₄ ²⁻ released from pyrite, Al ³⁺ and K ⁺ from host rock
Fifth	Ammoniojarosite (NH ₄)Fe ₃ (SO ₄) ₂ (OH) ₆	$3Fe^{3+} + 2SO_4^{2-} + NH_4^+ + 6H_2O \rightarrow (NH_4)Fe^{3+}_3(SO_4)_2(OH)_6 + 6H^+$	SO ₄ ²⁻ and Fe released from pyrite, and NH ₄ ⁺ from biological activity
	Tschermigite (NH ₄)Al(SO ₄) ₂ ·12H ₂ O	$Al^{3+} + 2(SO_4)^{2-} + NH_4^+ + 12 H_2O \rightarrow (NH_4)Al^{3+}(SO_4)_2 \cdot 12H_2O$	SO ₄ ²⁻ released from pyrite, Al ³⁺ from host rock, and NH ₄ ⁺ from biological activity

*Most of these reactions are well known and can be found in the geological literature.

**Mitchell (2002).

Figure 1

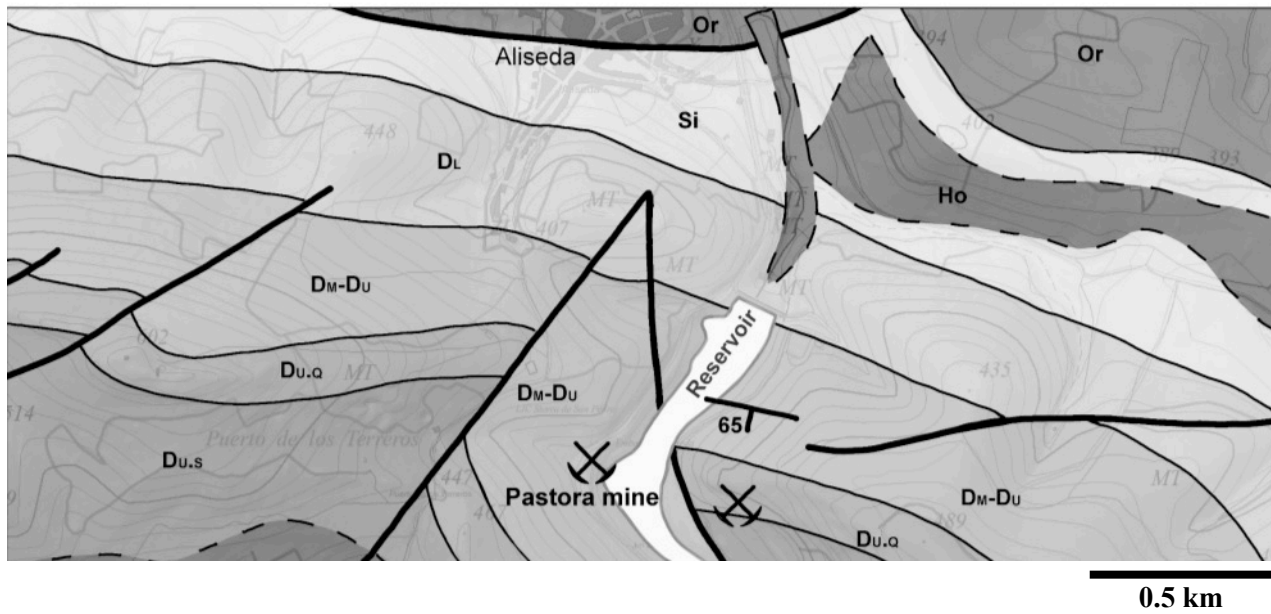


Figure 2

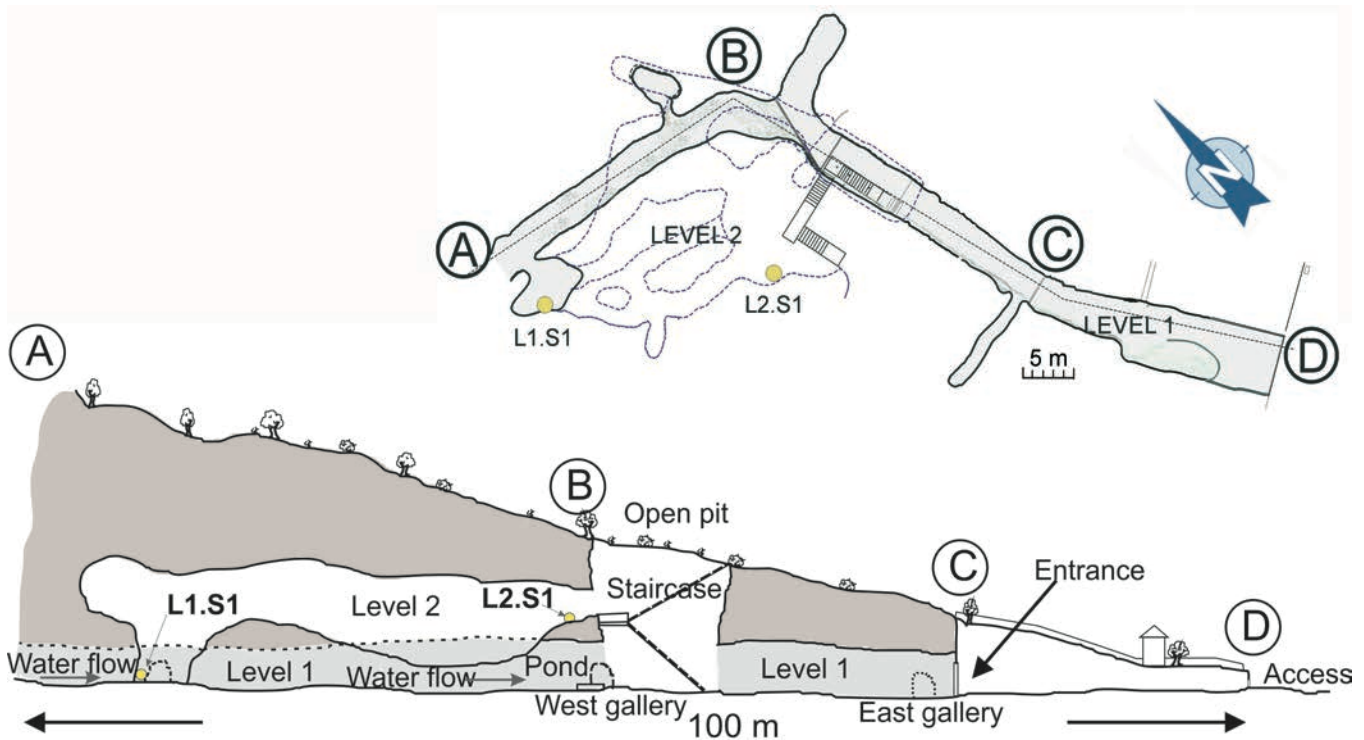


Figure 3

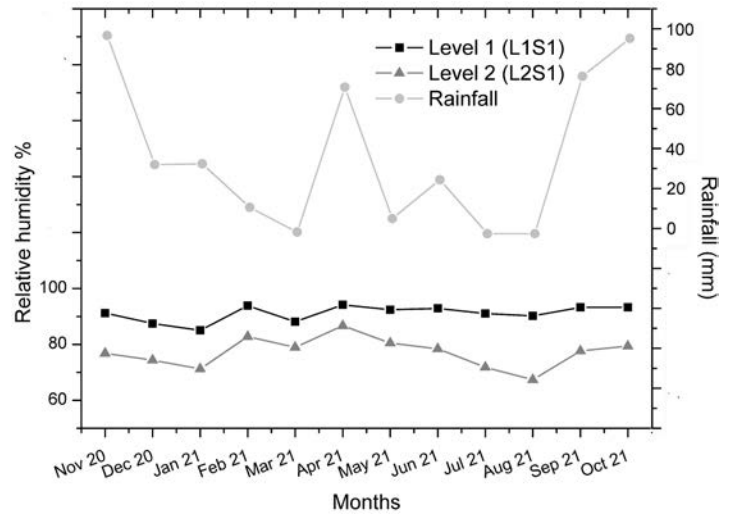
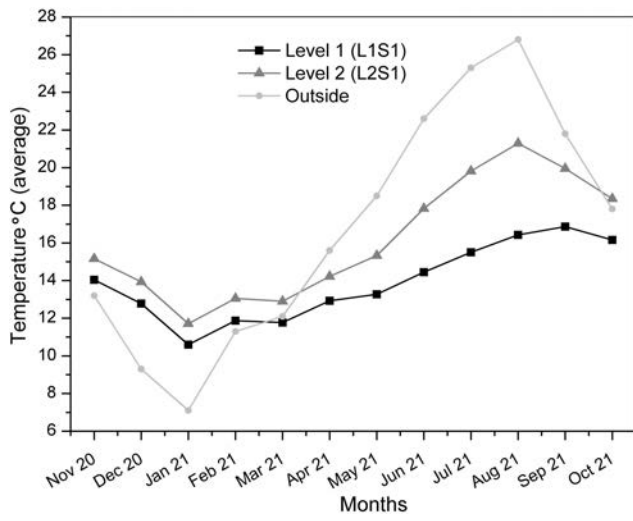


Figure 4

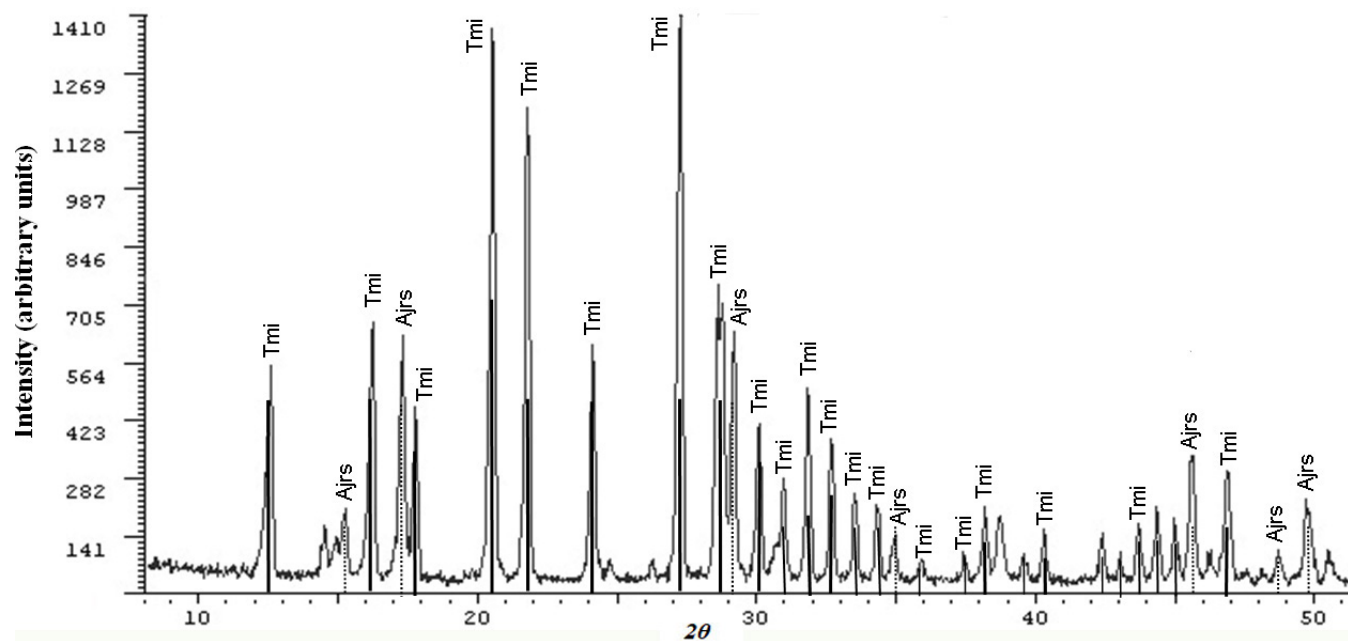


Figure 5

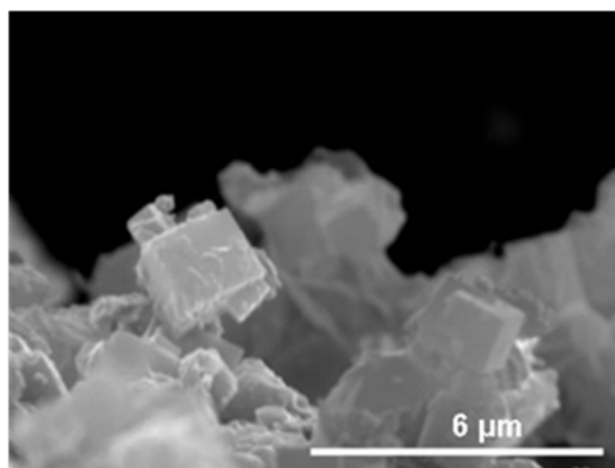
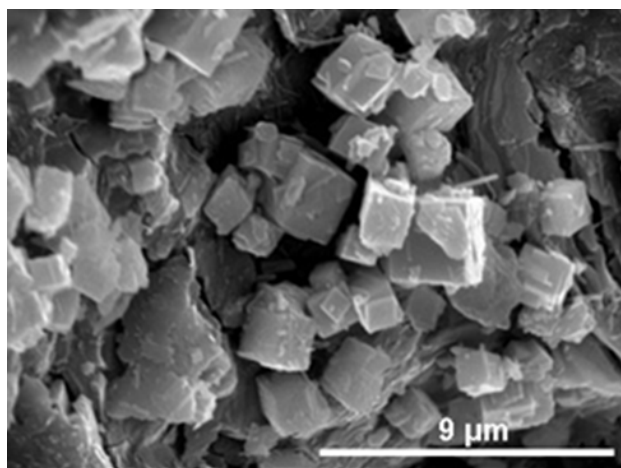


Figure 6

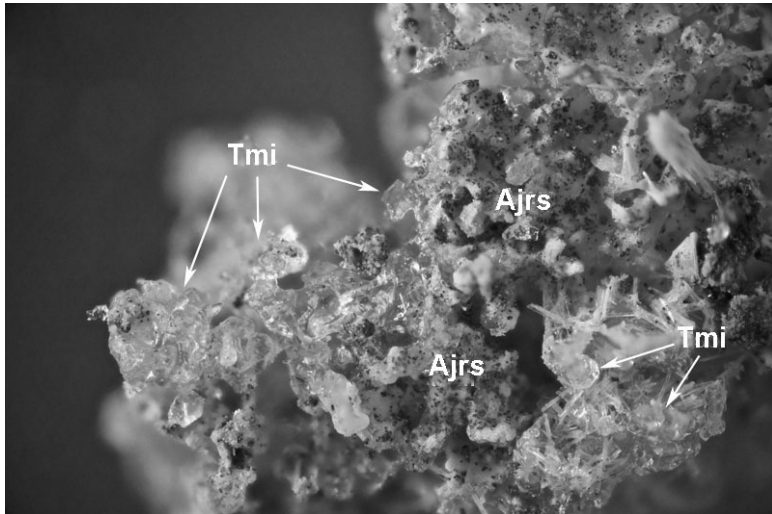


Figure 7

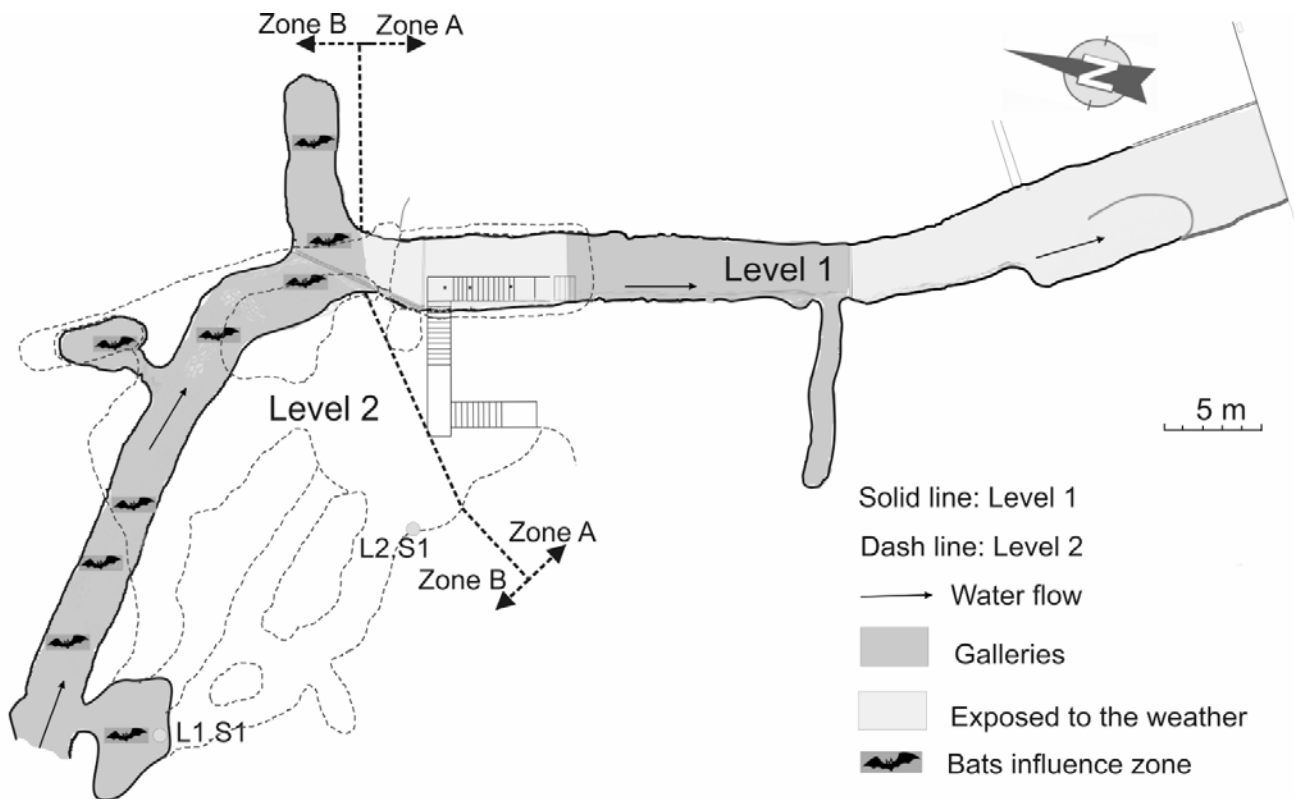


Figure 8

